Leptonic *CP* violation at neutrino telescopes

Davide Meloni

Dipartimento di Fisica "E. Amaldi", Universitá degli Studi Roma Tre, Via della Vasca Navale 84, 00146 Rome, Italy

Tommy Ohlsson

Department of Theoretical Physics, School of Engineering Sciences, KTH Royal Institute of Technology,
AlbaNova University Center, Roslagstullsbacken 21, 106 91 Stockholm, Sweden

With the advent of the recent measurements in neutrino physics, we investigate the role of high-energy neutrino flux ratios at neutrino telescopes for the possibility of determining the leptonic *CP*-violating phase δ and the underlying pattern of the leptonic mixing matrix. We find that the flux ratios show a dependence of $\mathcal{O}(10\%)$ on the *CP*-violating phase, and for optimistic uncertainties on the flux ratios less than 10%, they can be used to distinguish between *CP*-conserving and *CP*-violating values of the phase at 2σ in a nonvanishing interval around the maximal value $|\delta| = \pi/2$.

I. INTRODUCTION

Ever since 1998 with the results of Super-Kamiokande on atmospheric neutrinos [1], there is strong evidence for neutrino oscillations as the main mechanism for flavor transitions. Indeed, the fundamental parameters such as the two neutrino mass-squared differences Δm_{31}^2 and Δm_{21}^2 as well as the three leptonic mixing angles θ_{23}, θ_{12}, and θ_{13} are now determined with increasing accuracy. Recently, the third and last mixing angle θ_{13} has been measured by Daya Bay [2], but also Double Chooz, MINOS, RENO, and T2K have made important contributions [3–6]. All five experiments indicate that the value of the third mixing angle is around nine degrees. Thus, the value of this mixing angle is relatively large. This means that both the bimaximal and tribimaximal mixing patterns for leptonic flavor mixing have essentially been ruled out as zeroth-order approximations. Therefore, appropriate corrections must be taken into account to reconcile them with the experimental data. To this end, there remain two quantities for massive and mixed neutrinos that can be determined with oscillations: $\text{sgn}(\Delta m_{31}^2)$ and the Dirac *CP*-violating phase δ. The latter always appears in combination with θ_{13} in the leptonic mixing matrix as $\sin(\theta_{13}) \times \exp(\pm i\delta)$ and a nonzero value of θ_{13} means that it is possible to determine δ. The best options to measure δ are provided by accelerator experiments (e.g., NOvA and NuMI), future superbeams, beta beams, or even better a neutrino factory [7]. However, it will take a long time before such experiments are realized. In this work, we will therefore consider an alternative approach to determine δ by measuring neutrino flux ratios at neutrino telescopes. The generic example of such a telescope is IceCube [8], which exists and has the potential to measure flux ratios [9]. The dependence of flux ratios on the mixing parameters has been addressed in the literature where the

focus has been on the dependence on θ_{23} and θ_{13} [10–12], on δ [13], and on new physics effects [14].

The aim of this work is to illustrate the potential of neutrino telescopes to detect δ through the measurement of flux ratios after the first measurements of θ_{13}. For our numerical evaluations, we adopt the best-fit values and uncertainties for the mixing angles in the normal hierarchy (NH) quoted in Ref. [15], which are presented in Table I. Note that, although the flux ratios are not sensitive to the mass-squared differences, a somewhat dissimilar behavior between NH and inverted hierarchy could be drawn if the allowed ranges for the parameters were sizeably different. However, this is not the case for the 3σ ranges considered in this analysis.

II. NEUTRINO FLUX RATIOS

The averaged neutrino oscillations probabilities can be written as (see e.g., Ref. [10])

$$\langle P_{\alpha\beta} \rangle = \sum_{i=1}^{3} |U_{\alpha i}|^2 |U_{\beta i}|^2, \qquad (1)$$

where the quantities $U_{\alpha i}$ are elements of the leptonic mixing matrix U. Starting from the flux ratios at a source given by $\phi_{\nu_e}^0 : \phi_{\nu_\mu}^0 : \phi_{\nu_\tau}^0$, the neutrino fluxes arriving at a detector are sensitive to oscillations in vacuum and are then computed as

TABLE I. Results of a global analysis [15] in terms of best-fit values, 1σ, 2σ, and 3σ ranges for NH only. See also Ref. [16] for another global analysis.

Parameter	Best-fit value	1σ range	2σ range	3σ range
$\sin^2\theta_{12}/10^{-1}$	3.2	3.03–3.35	2.9–3.5	2.7–3.7
$\sin^2\theta_{13}/10^{-2}$	2.6	2.2–2.9	1.9–3.3	1.5–3.6
$\sin^2\theta_{23}/10^{-1}$	4.9	4.4–5.7	4.1–6.2	3.9–6.4
δ/π	0.83	0.19–1.37	$[0, 2\pi]$	$[0, 2\pi]$

$$\phi_{\nu_\beta} = \sum_{\alpha=e,\mu,\tau} \phi^0_{\nu_\alpha} \langle P_{\alpha\beta} \rangle = \sum_{\alpha=e,\mu,\tau} \phi^0_{\nu_\alpha} \sum_{i=1}^{3} |U_{\alpha i}|^2 |U_{\beta i}|^2.$$

(2)

For example, in the case $\phi^0_{\nu_e}: \phi^0_{\nu_\mu}: \phi^0_{\nu_\tau} = 1: 2: 0$, the fluxes are stemming from pion-beam sources (πS), whereas in the case $\phi^0_{\nu_e}: \phi^0_{\nu_\mu}: \phi^0_{\nu_\tau} = 0: 1: 0$, they come from muon-damped sources (μDS). Then, the flux ratios are defined as follows:

$$R_{\alpha\beta} = \frac{\phi_{\nu_\alpha}}{\phi_{\nu_\beta}}.$$

(3)

Note that the three flux ratios $R_{e\mu}$, $R_{e\tau}$, and $R_{\mu\tau}$ are not independent of each other, since two of them will give the third one. For example, using $R_{e\mu}(R_{e\tau})^{-1}R_{\mu\tau} \equiv 1$, we showed in Ref. [10] that, up to second order in small quantities (to be defined below), the following sum rule holds: $R_{e\mu} - R_{e\tau} + R_{\mu\tau} \simeq 1$. Given also the simplicity of their analytical expressions, we will choose to examine first the relevant features of $R_{e\mu}$ and $R_{\mu\tau}$. Notice that a more accessible variable from the experimental point of view is given by

$$R = \frac{\phi_{\nu_\mu}}{\phi_{\nu_e} + \phi_{\nu_\tau}} = R_{\mu e} \frac{1}{1 + R_{\tau e}} = (R_{e\mu})^{-1} \frac{1}{1 + (R_{e\tau})^{-1}},$$

(4)

which is obviously related to the "fundamental" $R_{\alpha\beta}$. We will take into account R in Sec. III C, when dealing with the issue of achievable precision for the flux ratios at neutrino telescopes. It is important to stress that the various flux ratios are experimentally accessible at different neutrino energies. For example, IceCube has an energy threshold of 100 GeV for detecting muon tracks, and $\sim$1 TeV for detecting electron-related and tau-related showers. At higher energies, above $\sim$1 PeV, electron-related electromagnetic showers and the tau-related hadronic showers can also be distinguished. Here, we do not consider such details and assume to work in the appropriate energy regime, where all relevant $R_{\alpha\beta}$ can be measured.

III. INVESTIGATION OF NEUTRINO FLUX RATIOS

A. Estimate of the uncertainties for pion-beam sources

Since the exact formulas for the flux ratios are quite cumbersome, we prefer to present our results expanding these ratios in the small parameters θ_{13}, $\delta_{23} = \theta_{23} - \pi/4$, and $\delta_{12} = \theta_{12} - \bar{\theta}_{12}$, $\bar{\theta}_{12}$ being the best-fit value for θ_{12}. No restrictions have been applied to δ, which means that the following formulas are valid to all orders in δ. In our discussion, it is enough to consider the expansions up to first order for $R_{e\mu}$ and $R_{e\tau}$ and second order for $R_{\mu\tau}$ (see Ref. [10] for a detailed discussion). We obtain

$$R_{e\mu} = 1 + \frac{3}{4}\cos(\delta)\sin(4\theta_{12})\theta_{13} - \frac{3}{2}\sin^2(2\theta_{12})\delta_{23},$$

$$R_{\mu\tau} = 1 + 2\cos^2(\delta)\sin^2(2\theta_{12})\theta_{13}^2$$
$$+ 2\cos(\delta)\sin(4\theta_{12})\theta_{13}\delta_{23} + [\cos(4\theta_{12}) + 7]\delta_{23}^2.$$

(5)

At this order of the perturbation theory, $R_{e\tau} = R_{e\mu}$. Notice also that no contributions from δ_{12} appear at the perturbative level considered above, so we expect that, given the current best-fit value on θ_{12}, the impact of δ_{12} is negligible. Inserting the best-fit values from Table I into Eq. (5), we can evaluate the numerical weight of each term in the expansions:

$$R_{e\mu} \sim 1 + 0.5\cos(\delta)\theta_{13} - 1.3\delta_{23} + \mathcal{O}(\delta_{ij}^2),$$

$$R_{\mu\tau} \sim 1 + 1.7\cos^2(\delta)\theta_{13}^2 + 1.3\cos(\delta)\theta_{13}\delta_{23} + 6.3\delta_{23}^2.$$

(6)

Numerically, $\delta_{12} \sim 0.05$, $\theta_{13} \sim 0.2$, and $\delta_{23} \sim 0.15$. Since δ_{23} always appears with the largest coefficient, we can easily deduce that the main uncertainty comes from the current error on θ_{23}. The contribution of θ_{13} is modulated by δ, so we expect no impact from it for $\cos(\delta) \sim 0$.

We verified all of these statements by computing the $R_{\alpha\beta}$'s as functions of δ, using exact expressions for the flux ratios. For the sake of illustration, we present in Fig. 1 the results obtained for both $R_{e\mu}$ and $R_{\mu\tau}$. In the upper plots, we show the behavior of the two flux ratios when θ_{13} is varied inside its 3σ range, whereas in the lower plots, we show the same for θ_{23}, with the not shown parameters fixed to their best-fit values given in Table I. These plots confirm the conclusions drawn from Eq. (5). Although not explicitly shown, the impact of θ_{12} is completely negligible for $R_{\mu\tau}$, whereas for $R_{e\mu}$, it is numerically comparable to that of θ_{13}.

As a next step, we evaluate all allowed values of the flux ratios considering the simultaneous variations of all parameters within their respective uncertainties as specified in Table I. The results are shown in Fig. 2 (upper plots), where we also show the present correlation between the two flux ratios (lower plot). In these plots, the bands indicate allowed regions where all parameters are varied within their respective 3σ ranges, whereas the solid and dashed curves have been obtained from the 2σ and 1σ ranges, respectively. Figure 2 deserves some more comments. Let us consider the allowed regions within the dashed curves, which can illustrate a possible situation when all mixing parameters (especially θ_{23}) will be known with better accuracy than today. In this case, the dependence of the flux ratios on δ is pronounced, since $R_{e\mu}$ has maximum and minimum values corresponding to the CP-conserving values $\delta = 0, \pm\pi$, respectively; at $\delta = \pm\pi$, $R_{e\mu} \in [0.83, 0.97]$ and at $\delta = 0$, $R_{e\mu} \in [0.96, 1.13]$. For $R_{\mu\tau}$, the δ dependence is more complicated, so that the
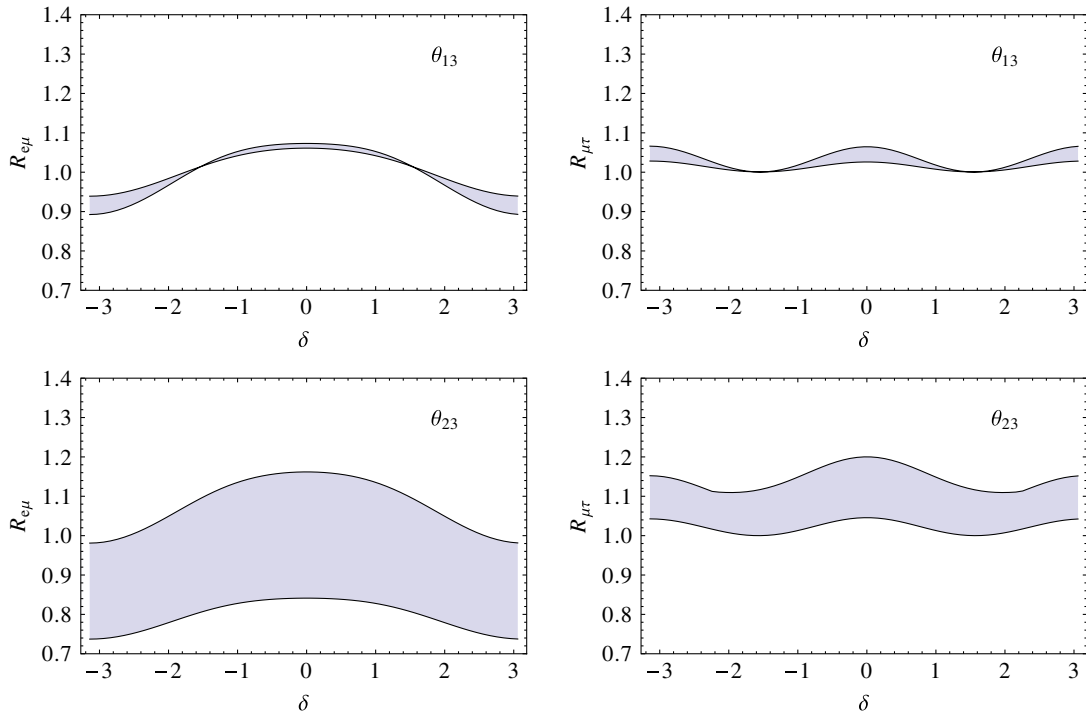
FIG. 1 (color online).   Variations of $R_{e\mu}$ (left plots) and $R_{\mu\tau}$ (right plots) as functions of δ when only the uncertainty on θ_{13} is taken into account (upper plots) or that on θ_{23} (lower plots).
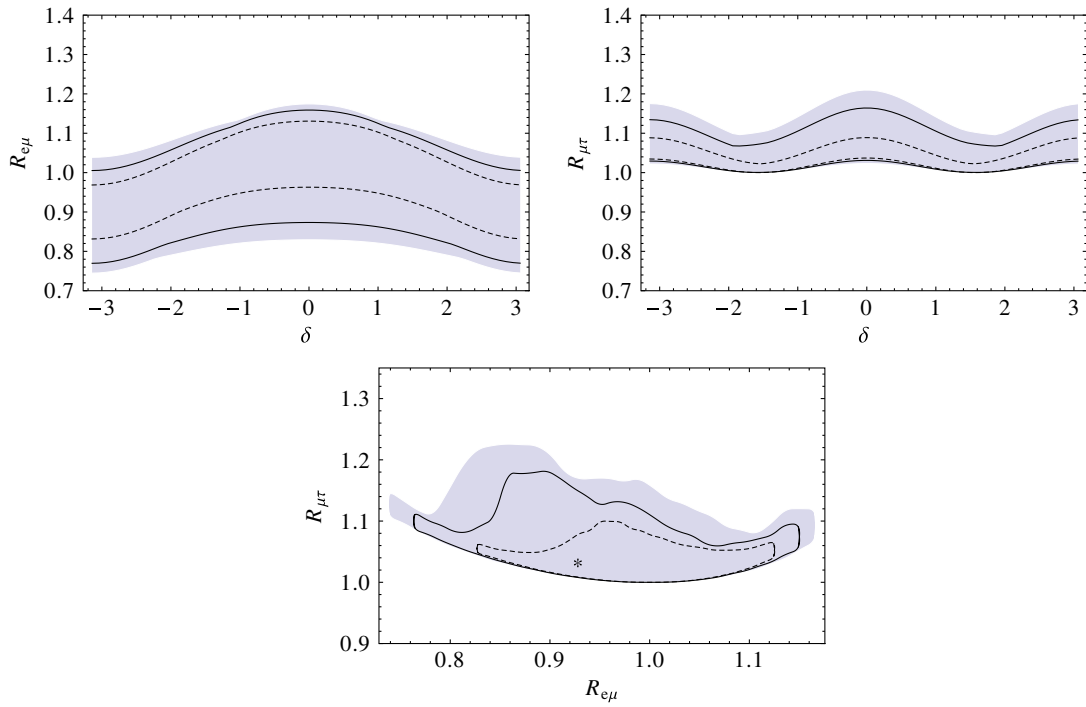

FIG. 2 (color online).   Total uncertainties on $R_{e\mu}$ (upper-left plot) and $R_{\mu\tau}$ (upper-right plot) as functions of δ when all other mixing parameters are varied within their 3σ errors. In the lower plot, we show the correlation between $R_{e\mu}$ and $R_{\mu\tau}$. Note that δ is left free in the interval $[-\pi, \pi]$.

flux ratio assumes similar values in [1.03, 1.09] for $\delta = 0$, $\pm \pi$, but $R_{\mu\tau} \in [1.00, 1.03]$ for $\delta = \pm \pi/2$.

If the errors on the mixing angles were larger, the dependence on δ would be less pronounced, but still enough to extract information on it (see below). Globally, we obtained the following ranges for the flux ratios:

$$R_{e\mu} \in [0.85, 1.18], \qquad R_{\mu\tau} \in [1.00, 1.21].$$

The correlation between the two flux ratios shown in the lower plot of Fig. 2 allows one to make consistency checks. Working in the absence of exotic processes (like neutrino decays), two simultaneous measurements of $R_{e\mu}$ and $R_{\mu\tau}$ should fall in these regions. For example, $R_{e\mu} \sim 0.8$ must be accompanied by $R_{\mu\tau} \sim 1.1$ to give $|\delta| \sim \pi$. It is interesting to note that the authors of Ref. [16] found a possible hint in favor of $\delta \sim \pi$. Thus, given all other best-fit values, these results—if they are confirmed—would imply $(R_{e\mu}, R_{\mu\tau}) = (0.93, 1.04)$, which is indicated by a "star" in the lower plot of Fig. 2.

B. Discussion on muon-damped sources

A similar study can be carried out for a muon-damped source, for which $\phi^0_{\nu_e} : \phi^0_{\nu_\mu} : \phi^0_{\nu_\tau} = 0: 1: 0$. Up to the first order in the small parameters, the relevant flux ratios read

$$\begin{aligned} R_{e\mu} = {} & \frac{4\sin^2(2\theta_{12})}{7 + \cos(4\theta_{12})} + \frac{64 \sin(4\theta_{12})}{[7 + \cos(4\theta_{12})]^2} \delta_{12} \\ & - \frac{4\cos(\delta)[-9 + \cos(4\theta_{12})]\sin(4\theta_{12})}{[7 + \cos(4\theta_{12})]^2} \theta_{13} \\ & + \frac{8[-9 + \cos(4\theta_{12})]\sin^2(2\theta_{12})}{[7 + \cos(4\theta_{12})]^2} \delta_{23}, \end{aligned}$$
$$R_{\mu\tau} = 1 - \frac{4\cos(\delta)\sin(4\theta_{12})}{7 + \cos(4\theta_{12})} \theta_{13} + \frac{8\sin^2(2\theta_{12})}{7 + \cos(4\theta_{12})} \delta_{23}. \tag{7}$$

Inserting the best-fit values of the mixing parameters, we obtain

$$R_{e\mu} = 0.6 + 1.1\delta_{12} + 0.7 \cos(\delta)\theta_{13} - 1.7\delta_{23} + \mathcal{O}(\delta^2_{ij}),$$
$$R_{\mu\tau} = 1.0 - 0.4 \cos(\delta)\theta_{13} + 0.9\delta_{23} + \mathcal{O}(\delta^2_{ij}), \tag{8}$$

where the uncertainty from δ_{12} is negligible at this order in $R_{\mu\tau}$. Some important differences arise when comparing the formulas in Eq. (8) with the corresponding ones in Eq. (5). In fact, $R_{e\mu}$ now obtains a leading dependence on δ_{12}, meaning that this flux ratio is more sensitive to the uncertainty of θ_{12} than the corresponding ratio for the 1: 2: 0 case. At the same time, $R_{\mu\tau}$ is corrected by the standard unit value by linear terms in θ_{13} and δ_{23}, which means that the fluctuations due to the current uncertainties on the mixing angles are more pronounced than before. These considerations are based on analytical formulas that have been verified numerically. As for the previous case, we found that the uncertainty on θ_{23} is the dominant source of
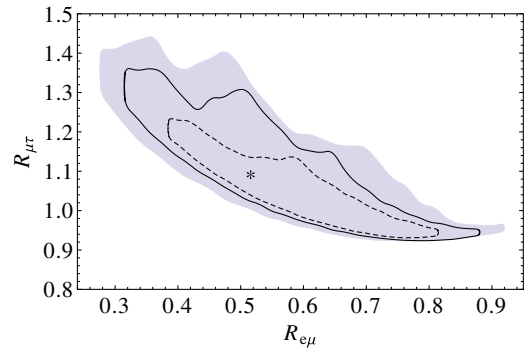

FIG. 3 (color online). Correlation between $R_{e\mu}$ and $R_{\mu\tau}$ for the 0:1:0 case obtained when the mixing parameters vary within their 1σ, 2σ, and 3σ ranges. Note that δ is left free in the interval $[-\pi, \pi]$.

error, and for $R_{e\mu}$, the error induced by θ_{12} is larger than the one given by θ_{13}. Besides these differences, the qualitative behavior of the flux ratios as functions of δ is similar to the ones shown in the upper plots of Fig. 2. On the other hand, the correlation between the two flux ratios is different from the previous case, so we display it in Fig. 3. As can be observed, there exists a "negative" correlation, extending for $R_{e\mu} \in [0.27, 0.92]$ and $R_{\mu\tau} \in [0.92, 1.42]$.

C. Potential to measure a nonvanishing *CP*-violating phase

Following Ref. [17], we study the potential of neutrino telescopes to distinguish between *CP*-conserving and *CP*-violating values of δ, using the possible measurements of R and $R_{e\tau}$ and also the capability to differentiate between πS and μDS sources. This is a difficult task, as was outlined in Ref. [9], especially if the uncertainties on the considered flux ratios are large. For the sake of completeness, we present the dependence on δ for R and $R_{e\tau}$ computed at the best-fit values of θ_{ij} for both πS and μDS sources:

$$\begin{aligned} R^{\pi S} &\sim \frac{3}{1.99 + 0.03 \cos(\delta)} - 1, \\ R^{\pi S}_{e\tau} &\sim \frac{19.1 + \cos(\delta)}{18.7 - 0.47 \cos(\delta) - 0.21 \cos(2\delta)}, \\ R^{\mu DS} &\sim \frac{1}{0.61 + 0.03 \cos(\delta)} - 1, \\ R^{\mu DS}_{e\tau} &= \frac{8.94 + \cos(\delta)}{14.3 + 0.02 \cos(\delta) - 0.21 \cos(2\delta)}. \end{aligned} \tag{9}$$

The coefficients of the $\cos(\delta)$ terms are small and relevant for the *CP*-conserving values. In addition, there are no preferred sources in the determination of δ, since the δ dependence in the flux ratios built from πS and μDS is not really dissimilar.

To evaluate how $\delta = 0$ can be distinguished from other nonvanishing values, we construct a χ^2 function
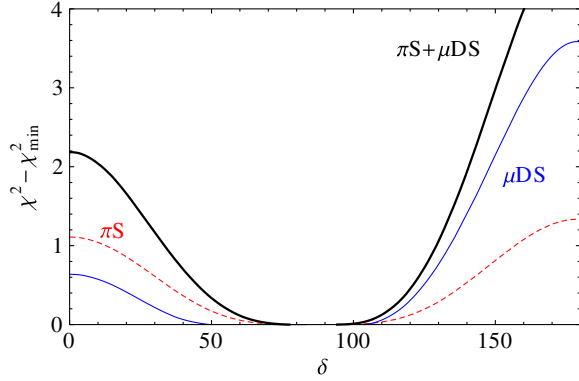
FIG. 4 (color online). $\chi^2 - \chi^2_{\min}$ as a function of δ, after minimizing over all nondisplayed parameters. The three curves refer to πS (dashed curve), μDS (thin solid curve), and the sum of both (thick solid curve).

$$\chi^2 = \left[\frac{R^{\exp} - R(\theta_{ij}, \delta)}{\sigma_R}\right]^2 + \left[\frac{R_{e\tau}^{\exp} - R_{e\tau}(\theta_{ij}, \delta)}{\sigma_{R_{e\tau}}}\right]^2, \quad (10)$$

where $R^{\exp}$ and $R_{e\tau}^{\exp}$ are R and $R_{e\tau}$ evaluated at the best-fit points for θ_{ij} as given in Table I. We consider the possibility of having the sum of both contributions from πS and μDS sources. In the minimization procedure, we marginalize over all parameters but δ. As an illustrative example, we show in Fig. 4 the case where $\delta = \pi/2$. In the χ^2 function, we assume 5% error on the flux ratios. As expected, the combination of both πS and μDS sources gives the best resolution for δ. In particular, the χ^2 function does not touch the CP-conserving values $\delta = (0, \pi)$ at 2σ, so maximal CP violation can be distinguished from CP conservation. This can be repeated for every input value of δ; at a given confidence level and flux ratio uncertainty, there exists a range of phases for which the χ^2 function does not touch $\delta = (0, \pi)$; the fraction of such points over the whole $[0, \pi]$ range defines a CP fraction that serves to illustrate the goodness of the neutrino telescope to access CP violation. The result is reported in Fig. 5, where we display the 2σ CP fraction in terms of the uncertainty $\sigma_R = \sigma_{R_{e\tau}} = \sigma$, ranging from 1 to 10%, obtained using the χ^2 function defined in Eq. (10). We have considered four cases; the long-dashed curve refers to the case in which all mixing parameters but δ are fixed to their best-fit values and all neutrino sources are taken into account. It is clear that the best performance is reached when the maximum amount of information is collected (i.e., the sum of the sources). However, such performances are limited to $\sigma \lesssim 0.065$. Even considering infinite precision on the mixing angles, the CP fraction is nonvanishing only for $\sigma \lesssim 0.07$. This is
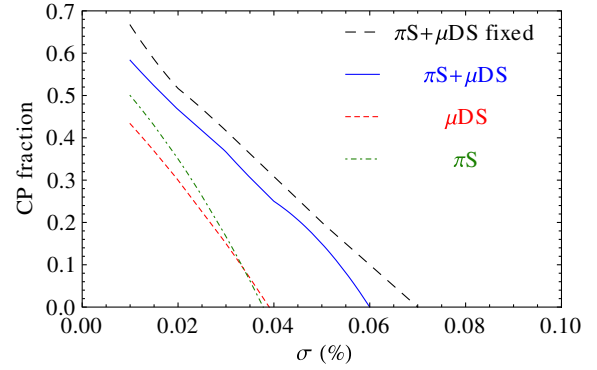

FIG. 5 (color online). 2σ CP fraction estimate as a function of the common flux ratio uncertainty. The four cases correspond to $\pi S + \mu DS$ (solid and long-dashed curves), μDS (dashed curve), and πS (dotted-dashed curve).

the consequence of the mild δ dependence on the flux ratios in Eq. (9). Nevertheless, since astrophysical high-energy sources have not been observed so far, a more promising possibility would be to combine future neutrino telescope data with other future experimental data (from e.g., NOvA), which should have some sensitivity to the octant of θ_{23}, and thus reducing the intrinsic uncertainties on the flux ratios.

IV. SUMMARY AND CONCLUSIONS

In this paper, we have analyzed the potential of neutrino telescopes to access the leptonic CP-violating phase δ. We have derived expansions for the flux ratios $R_{\alpha\beta}$ up to the first (and second) order in small parameters, explicitly showing their dependence on δ, for both kinds of high-energy neutrino sources, i.e., πS and μDS sources. It turns out that the uncertainty on θ_{23} affects the global (theoretical) error on the flux ratios the most. Considering both kinds of sources, we have shown that a 10% of CP fraction can still be obtained with a 5.5% uncertainty on $R_{\alpha\beta}$. We urge IceCube to measure the flux ratios, since such a measurement could provide the first hints on the value of δ.

ACKNOWLEDGMENTS

[1] Y. Fukuda *et al.* (Super-Kamiokande Collaboration), Phys. Rev. Lett. **81**, 1562 (1998).

[2] F. P. An *et al.* (Daya Bay Collaboration), Phys. Rev. Lett. **108**, 171803 (2012).

[3] Y. Abe *et al.* (Double Chooz Collaboration), Phys. Rev. Lett. **108**, 131801 (2012).

[4] P. Adamson *et al.* (MINOS Collaboration), Phys. Rev. Lett. **107**, 181802 (2011).

[5] J. K. Ahn *et al.* (RENO Collaboration), Phys. Rev. Lett. **108**, 191802 (2012).

[6] K. Abe *et al.* (T2K Collaboration), Phys. Rev. Lett. **107**, 041801 (2011).

[7] S. Choubey, *et al.*, Report No. IDS-NF-017.

[8] IceCube Neutrino Observatory, http://icecube.wisc.edu/.

[9] P. Lipari, M. Lusignoli, and D. Meloni, Phys. Rev. D **75**, 123005 (2007); G.-R. Hwang and K. Siyeon, Phys. Rev. D **78**, 093008 (2008); S. Pakvasa, W. Rodejohann, and T. J. Weiler, J. High Energy Phys. 02 (2008) 005.

[10] D. Meloni and T. Ohlsson, Phys. Rev. D **75**, 125017 (2007).

[11] P. D. Serpico, Phys. Rev. D **73**, 047301 (2006); S. Choubey, V. Niro, and W. Rodejohann, Phys. Rev. D **77**, 113006 (2008); Z.-z. Xing and S. Zhou, Phys. Lett. B **666**, 166 (2008); A. Esmaili and Y. Farzan, Nucl. Phys. **B821**, 197 (2009).

[12] Z.-z. Xing, Phys. Rev. D **74**, 013009 (2006); W. Rodejohann, J. Cosmol. Astropart. Phys. 01 (2007) 029; D. Majumdar and A. Ghosal, Phys. Rev. D **75**, 113004 (2007); Z.-z. Xing, arXiv:1205.6532 [Phys. Lett. B (to be published)].

[13] P. D. Serpico and M. Kachelrieß, Phys. Rev. Lett. **94**, 211102 (2005); W. Winter, Phys. Rev. D **74**, 033015 (2006).

[14] M. Blennow and D. Meloni, Phys. Rev. D **80**, 065009 (2009); R. L. Awasthi and S. Choubey, Phys. Rev. D **76**, 113002 (2007); M. Maltoni and W. Winter, J. High Energy Phys. 07 (2008) 064; P. Mehta and W. Winter, J. Cosmol. Astropart. Phys. 03 (2011) 041.

[15] D. V. Forero, M. Tórtola, and J. W. F. Valle, arXiv:1205.4018.

[16] G. L. Fogli, E. Lisi, A. Marrone, D. Montanino, A. Palazzo, and A. M. Rotunno, Phys. Rev. D **86**, 013012 (2012).

[17] K. Blum, Y. Nir, and E. Waxman, arXiv:0706.2070.